

1 **Assembly of a Parts List of the Human Mitotic Cell Cycle Machinery**

2

3 Bruno Giotti¹, Sz-Hau Chen¹, Mark W. Barnett¹, Tim Regan¹, Tony Ly², Stefan Wiemann³, David
4 A. Hume¹ and Tom C. Freeman^{1†}

5

6 ¹. The Roslin Institute and ². School of Biological Sciences, University of Edinburgh, Easter Bush,
7 Midlothian, Scotland, UK EH25 9RG.

8 ³. Molecular Genome Analysis (B050), Deutsches Krebsforschungszentrum, Im Neuenheimer
9 Feld 580, 69120 Heidelberg, Germany.

10

11 [†]To whom correspondence should be addressed.

12

13 **Abstract**

14 The set of proteins required for mitotic division remains poorly characterised. Here, an
15 extensive series of correlation analyses of human and mouse transcriptomics data was
16 performed to identify genes strongly and reproducibly associated with cells undergoing S/G2-
17 M phases of the cell cycle. In so doing, a list of 701 cell cycle-associated genes was defined
18 and shown that whilst many are only expressed during these phases, the expression of others
19 is also driven by alternative promoters. Of this list, 496 genes have known cell cycle functions,
20 whereas 205 were assigned as putative cell cycle genes, 53 of which are functionally
21 uncharacterised. Among these, 27 were screened for subcellular localisation revealing many
22 to be nuclear localised and at least four to be novel centrosomal proteins. Furthermore, 10
23 others inhibited cell proliferation upon siRNA knockdown. This study presents the first
24 comprehensive list of human cell cycle proteins, identifying many new candidate proteins.

25 Introduction

26 Mitotic cell division is a process common to all eukaryotic organisms and achieved through a
27 highly orchestrated series of events classified into four sequential phases: G₁ (gap phase), S
28 (DNA replication), G₂ and M (mitosis). The concerted action of hundreds of proteins is required
29 to drive the process through to a successful conclusion, many of which are expressed in a
30 phase-specific manner. They mediate processes such as DNA replication and repair,
31 chromosome condensation, centrosome duplication and cytokinesis. Dysregulation or
32 mutation of genes encoding proteins essential for high fidelity DNA replication, is often
33 associated with disease, in particular cancer^{1,2}. Accordingly, known components of this system
34 are important therapeutic targets³ and novel components might present new therapeutic
35 opportunities.

36
37 Many of the key proteins required for mitotic division are known from studies in model
38 organisms including yeast, as well as mammalian cells^{4,5}. With the aim of identifying all the
39 components of the system, high content analysis platforms have been utilised. For example
40 RNAi screens⁶⁻⁸, CRISPR/Cas9⁹, proteomics^{10,11,12} studies have all proposed lists of cell cycle
41 genes/proteins but a consensus between studies has not emerged. In particular, genome-wide
42 transcriptomics studies¹³⁻¹⁹ have identified sets of transcripts sequentially regulated during
43 the cell cycle phases in multiple species but comparison of results from four studies of
44 different human cell lines identified only 96 genes in common¹⁵. Our reanalysis of these data,
45 taking account of some of the technical variables, suggested that the true concordance of the
46 cell cycle transcriptional network across cell types is much greater²⁰. Furthermore, our
47 analyses of large collections of tissue and cell transcriptomics data commonly identify a large
48 cluster of cell cycle transcripts whose expression is elevated in cells or tissues with a high
49 mitotic index²¹⁻²⁵.

50
51 We report here on a data driven curation exercise aimed at identifying the cohort of genes
52 up-regulated in all human cell types from the G₁/S boundary through to the completion of M
53 phase (S/G₂-M). There are of course, many growth-associated transcriptional regulatory
54 events including activation of cyclins, cyclin-dependent kinases and E2F transcription factors,
55 that occur during G₁ and are a precondition for entry into S phase²⁶, but these are not the
56 focus of this study. We monitored genome-wide gene expression in primary human dermal
57 fibroblasts (NHDF) cells as they synchronously enter the cell cycle from a resting state (G₀).
58 Using network co-expression analysis and clustering of the data, we identified a cell cycle-
59 enriched cluster associated with S/G₂-M phases. To refine this initial list, we identified those
60 genes that were robustly co-expressed when their transcription was examined across multiple
61 different human primary cell types in the promoter-based FANTOM5 transcriptional data set²⁷
62 and in synchronised murine fibroblasts. Manual curation of these data resulted in a list of 701
63 genes strongly associated with the S/G₂-M phase transcriptional network. Of these, 496
64 encode proteins with known functions within cell division, 145 of which were not identified in
65 any of the previous human cell cycle transcriptomics studies. Of the remaining 205 genes, 53
66 encode functionally uncharacterised proteins. To further validate this discovery set, we

67 examined their expression across a range of human tissues and in mouse embryonic tissues
68 during development. We also performed functional assays including protein localisation by
69 over-expression of GFP-tagged proteins and knockdown by RNAi.

70

71 **Methods**

72

73 **Cell culture and synchronization**

74 Primary human dermal fibroblasts (NHDF) isolated from neonate foreskins (gifted by Dr Finn
75 Grey, University of Edinburgh, UK) were plated on 175 cm² tissue culture flasks (Thermo
76 Fisher, Perth, UK) at density of 6x10³ cells/cm². Cells were cultured in DMEM (Sigma-Aldrich,
77 Missouri, US) with 10% (v/v) foetal calf serum (FCS) (GE Healthcare, Little Chalfont, UK) and
78 antibiotics (25 U/ml penicillin and 25 µg/ml streptomycin (Life technologies, Paisley, UK).
79 Starvation-induced synchronisation was achieved by replacing full medium with DMEM
80 containing 0.5% FCS for 48 h in accordance with published methods²⁸. After this time, medium
81 was replaced with DMEM containing 10% FCS promoting the synchronised entry of the NHDF
82 back into the cell cycle. Similarly, mouse embryonic fibroblasts (MEF) were cultured in 175
83 cm² tissue culture flasks (Thermo Fisher) at a density of 6,000 cells/cm² in DMEM with 10%
84 FCS and the same protocol followed as for NHDF synchronisation.

85 In both cases, cell synchronisation was assessed after 48 h of serum starvation and at various
86 time points following the re-addition of complete medium using a BD LSR Fortessa X-20 flow
87 cytometer (BD Biosciences, San Jose, CA, US) with propidium iodide staining. Unsynchronised
88 populations were evaluated to assess the degree of synchronisation achieved. For protein
89 localisation assays, 1x10⁵ HEK293T cells were grown in DMEM (Sigma-Aldrich) medium plus
90 10% FCS, 1% Glutamax (Gibco, Gaithersburg, US), 1% non-essential amino acids (Gibco) and
91 25 Units/ml penicillin/streptomycin on 13 mm glass coverslips previously coated with poly-L-
92 lysine (0.1 mg/ml) in each well of a 24-well plate. Cells were grown until coverage of
93 approximately 70% was obtained. To increase percentage of cells undergoing mitosis, HEK293
94 were reversibly blocked at the G₂/M boundary with RO3306, as described previously²⁹.

95

96 **Microarray preparation**

97 Two human microarray datasets were generated using normal human foreskin fibroblasts
98 (NHDF). For the first microarray experiment duplicate samples were taken at 6 h intervals over
99 a 48 h period (24 samples in total including unsynchronised control cells cultured in parallel
100 and harvested at 0 and 24 h). In a second independent experiment, samples were collected at
101 1 and 2 h following re-addition of complete medium, and then every 2 h for a 24 h period (16
102 samples in total including two control samples). In a third microarray experiment using mouse
103 fibroblasts, MEF samples were collected at 0, 0.5, 1, 2 h following re-addition of complete
104 medium and then every 2 h for a 30 h period (24 samples in total including replicates for 0,
105 12, 18, 24 h samples and unsynchronised control samples). For all experiments described
106 above total RNA was isolated using the RNeasy Mini Kit (QIAGEN, Manchester, UK) according
107 to manufacturer's instructions. cDNA was generated by the reverse transcription of total RNA
108 (500 ng) using the Ambion WT Expression Kit (Life technologies), fragmented and then labelled

109 by TdT DNA labelling reagent using GeneChip® WT Terminal Labelling Kit (Affymetrix,
110 Buckinghamshire, UK) according to manufacturer's instructions. Samples were hybridized to
111 Affymetrix Human Gene 1.1-ST Arrays for both NHDF time course experiments and to the
112 Mouse Gene 2.0 ST Arrays for the MEF experiment using an Affymetrix GeneAtlas system. For
113 cross-validation the Fantom5 (F5) primary cell atlas of human promoter expression²¹ was
114 used, including 495 samples from about 100 human primary cell types. The data is publicly
115 available at <http://fantom.gsc.riken.jp/5/>³⁰.

116

117 **Data pre-processing**

118 Raw data (.cel files) derived from the three microarray experiments were pre-processed using
119 *Bioconductor* (www.bioconductor.org). The package *ArrayQualityMetrics* was used to
120 perform QC on the data. All arrays passed the various tests carried out by the package and
121 expression levels were normalised using Robust Multiarray Averaging (RMA) normalisation
122 using the *Oligo* package. The two normalised NHDF datasets were also adjusted with the batch
123 correction algorithm ComBat³¹ to adjust for variations in the average intensity between
124 experiments. Low intensity signal probesets (< 20) were removed (a total of 9,408 probesets).
125 Likewise, a filtering of low-end signal was applied on the FANTOM5 primary cell atlas removing
126 promoters with <5 tags per million (TPM) reads. Probe set annotations were retrieved with
127 the *hugene11transcriptcluster.db* package for the human data and with
128 *mogene20sttranscriptcluster.db* package for the mouse data. Mouse to human orthologues
129 were retrieved from the web resource Mouse Genome Informatics (MGI)
130 (<http://www.informatics.jax.org/>).

131

132 **Network analysis**

133 The NHDF, FANTOM5 (primary cell and mouse development datasets)²⁷, Tissue atlas dataset³²
134 and MEF datasets were subjected to network-based correlation analyses. Data was loaded
135 into the tool Miru (Kajeka Ltd., Edinburgh, UK) and Pearson correlation matrices were
136 calculated comparing expression profiles between individual samples or genes, and these
137 were used as the basis to construct co-expression networks as described previously²³.
138 Correlation thresholds for all analyses were set to allow minimal contribution of random
139 correlations to the analyses. These were based on a comparison of the correlation
140 distributions of the experimental datasets vs. permuted measurements from 2,000 randomly
141 selected measurements. Values selected also minimised the number of edges whilst
142 maintaining a maximum number of nodes (Figures S1-2). The two NHDF time-course
143 experiments were analysed together. A correlation network was constructed using a
144 threshold of $r \geq 0.88$ and the graph clustered to identify co-expression modules of genes with
145 a broadly similar expression pattern using the MCL clustering algorithm³³ with the inflation
146 value (which controls the granularity clustering) set to 1.3 (MCLi = 1.3). Clusters of genes
147 whose expression varied for technical reasons, i.e. profile associated with a batch or
148 experiment, were removed. The correlation network of the remaining data comprised of
149 4,735 nodes (probesets) connected by 153,809 edges. Using different inflation values the
150 network was divided into a few (MCLi 1.3) or many (MCLi 2.2) clusters of transcripts.

151 Transcripts within the S/G2-M cluster (cluster 3) plus all nodes immediately adjacent to them
152 (n+1), were then selected for further analysis. The node walk expansion was to capture a
153 number of similarly expressed genes on the periphery of the main cluster. Entrez IDs of the
154 cell cycle-associated transcripts identified in the NHDF data were used to subset the FANTOM5
155 primary cell atlas, prior to network analysis. The subset FANTOM5 primary cell atlas data was
156 then parsed at $r \geq 0.5$ and clustered at MCLi = 1.7. The MEF time-course data was parsed at r
157 ≥ 0.88 and the resultant networks clustered using MCLi = 2.2. The Tissue Atlas and FANTOM5
158 mouse development datasets were subset for the curated S/G2-M gene list, plotted at $r \geq 0.5$,
159 and clustered at MCLi 3.2 and 1.7, respectively.

160

161 **Assembly of evidence and annotation of the cell cycle ‘parts list’**

162 In assembling a list of cell cycle genes we have sought to bring together various sources of
163 evidence to support this association. This includes whether they were implicated by the
164 current studies of their expression in experiments performed on NHDF, MEF or human
165 primary cell atlas, previous transcriptomics studies on human cells^{13,14,16,18,34,35}, the Mitochek
166 database³⁶ and human protein atlas (HPA)³⁷ resource, and finally, our own functional assays.
167 Furthermore, we examined evidence from the literature as well as annotation and pathway
168 resources to provide, where possible, a functional grouping and annotation for each gene.
169 This was carried out by retrieving UniprotKB biological process terms (UniprotKB *keywords*)
170 and when none were found for a given gene, annotation was supplemented from other
171 sources, namely Gene Ontology³⁸ and Reactome³⁹. These efforts were backed up by extensive
172 review of the published literature. The full list of genes with their corresponding functional
173 annotation can be found in S1 Table. Based on this work, genes were further classified based
174 on evidence of their involvement in cell cycle: The *Known* group defines genes for which there
175 is robust evidence of their involvement in one of the pathways associated with the cell cycle,
176 whereas the *Putative* group includes genes for which there is little or no direct evidence of
177 them being involved in the cell cycle. This group also includes a number of functionally
178 uncharacterised genes. Finally, a simple confidence score was used to order the cell cycle list
179 based on the weight of evidence supporting a gene’s involvement in the cell cycle; One point
180 was awarded to all genes for each line of evidence supporting their association with the cell
181 cycle, i.e. they were identified by the current or five previous human transcriptomics
182 studies^{13,14,16,18,34}, their knockdown generated a mitosis-related phenotype in the current
183 Mitochek screen³⁶ and whether the gene has been associated with a cell cycle-related
184 phenotype in human and mouse^{40,41}.

185

186 **Gene Ontology and motifs enrichment analysis**

187 GO enrichment analyses were conducted with the Database for Annotation, Visualization and
188 Integrated Discovery (DAVID, v6.8), a web-based tool for Gene Ontology enrichment analysis
189 (<http://david.abcc.ncifcrf.gov/>). Gene sets within the clusters generated by the MCL algorithm
190 were analysed for GO_BP terms using the Functional Annotation clustering tool. Motifs
191 enrichment analysis was conducted using HOMER⁴² through the CAGED-oPOSSUM web tool
192 ⁴³. Genomic loci of the cell cycle-associated promoters were inputted in the software.

193 Enrichments for known motifs were searched between 1,000 bp upstream and 300 bp
194 downstream from the TSS.

195

196 **RTCA analysis following gene knockdown by RNAi**

197 NHDF cells were cultured in Dulbecco Modified Eagle Medium (DMEM, Sigma-Aldrich) with
198 10% v/v (foetal bovine serum (FBS, GE Healthcare) and 25 U/ml penicillin and 25 µg/ml
199 streptomycin (Life technologies). The xCELLigence (Roche, Penzberg, Germany) real time cell
200 analyser (RTCA) system was used to monitor the effect of gene knockdown on cell impedance,
201 taken as a proxy for cell proliferation. Background impedance for the E-plates 96 (ACEA
202 Biosciences, San Diego, US) was standardized by the addition of culture medium (DMEM with
203 10% FBS, and 25 U/ml penicillin and 25 µg/ml streptomycin) following the manufacturer's
204 instructions. Following trypsination, cells were seeded at density of 6,000 cells/cm² in each
205 well of the 96 well E-plates with the additional of 100 µl complete medium. Baseline levels of
206 cell impedance index recorded and 24 h later, esiRNA transfection esiRNAs (Sigma-Aldrich)
207 was performed while plates were undocked from the RTCA station. Transfection of esiRNA
208 was carried out using the transfection reagent SilenceMag (OZ bioscience, Marseille, France).
209 esiRNA was combined with 3.3 µl SilenceMag and 3.0 µl H₂O, and then mixed with antibiotic-
210 free medium in a final volume of 100 µl and a concentration of 50 nM esiRNA per well.
211 Complete medium was then replaced with the transfection mix, placed on magnetic plates
212 (OZ bioscience) for 30 min in the incubator under the condition of 5% CO₂ at 37°C. The
213 transfection mix was then replaced with 200 µl complete medium before placing the plates
214 back to the RTCA system. Cells were then incubated monitoring the cell impedance index
215 every 15 min for 200 sweeps in first stage, 30 min for 200 sweeps in second stage, and
216 continued at 60 min intervals for 100 sweeps in final stage. Time series cell impedance indices
217 were extracted at regular time intervals. Negative controls were tested across each plate used
218 to screen known (39) and potentially novel cell cycle-associated genes (22). At the time of
219 screen a number of the known genes were considered uncharacterised. Each assay was based
220 on results gained from running three replicate assays per plate, and repeated on three
221 separate runs. The raw dataset was exported as a cell impedance (CI) index with rows named
222 by N time points (measurement time points at 30 min intervals following the transfection) and
223 columns named by well of samples. Statistical analysis of the data was performed using the R
224 package "RTCA" to transform cell-impedance values into cell-index growth rate (CIGR) at
225 regular time intervals during the measurement time⁴⁴. For scoring of the effect of gene
226 silencing- induced proliferation arrest, the package "cellHTS2" was used to normalize average
227 CIGR across samples⁴⁵.

228

229 The library of esiRNAs (endoribonuclease-prepared short interfering RNAs, Sigma-Aldrich)
230 employed here has been described elsewhere^{46,47}. Negative control esiRNA reagents against
231 sucrose isomaltase (*SI*), a gene not expressed by fibroblasts and collagen 1A2 (*COL1A2*), a gene
232 expressed by fibroblasts but not associated with cell division. All control esiRNA reagents were
233 used in each assay to verify the lack of non-specific effects of esiRNA treatment.

234

235 **Clone preparation**

236 Entry clones in pDONR223 and containing open reading frames for candidate genes were
237 sourced from the ORFeome collection⁴⁸. 50-150 ng of each entry clone was combined with
238 150 ng destination vector pcDNA-DEST47 or pcDNA-DEST53 (Life technologies) and 2 µl LR
239 Clonase II enzyme mix (Life technologies). The reaction was incubated at 25°C for 1 h. 1 µl (2
240 µg/µl) proteinase K was added to terminate the reaction, incubating for 10 min at 37°C. 2 µl
241 of the recombination reaction was added to chemically competent DH5α bacterial cells on ice
242 and incubated for 20 min. DH5α cells were subjected to heat shock for 45 sec at 42°C followed
243 by 2 min on ice. 1 ml SOC medium was added and incubated at 37°C with aeration. Cells were
244 centrifuged at 2,000 rpm and resuspended in 100 µl LB before plating out on LB plates with
245 100 µg/ml ampicillin. Plates were incubated at 37°C overnight.

247 **DNA transfection and Confocal Microscopy**

248 Transfection of HEK293 cells with Gateway destination clones and K2 transfection system
249 (Biontex Laboratories, Munchen, Germany) was performed following manufacturer's
250 instructions. Following optimisation studies, 1 µg of expression plasmid and 2 µl of the
251 transfection reagent were diluted in 500 µl in each well (24-well plate). For GFP fluorescence
252 protein imaging, cells were fixed in 4% paraformaldehyde and labelled for 30 min with Texas
253 RedX Phalloidin (1:40) (Invitrogen) and then stained for 5 min in 300 nM DAPI. For centrosomal
254 staining, polyclonal anti γ -tubulin antibody (Sigma-Aldrich) was used. Alternatively, a
255 polyclonal antibody anti α -tubulin (Abcam, Cambridge, England) was used to stain
256 microtubules during the formation of mitotic spindles. Fixation was carried out by applying
257 300 µl of cooled methanol per well for 2 min on ice. Cells were washed three times with PBS
258 and then blocked with 5% goat serum (Sigma-Aldrich) and 0.1% Triton in PBS for 1 h. Primary
259 antibodies were then diluted accordingly in blocking solution, applied on coverslips and
260 incubated either overnight at 4°C or for 2 h at room temperature. Cells were then washed
261 three times for 1 h with PBS. The secondary antibody was diluted in blocking solution (1:500),
262 applied on coverslips and incubated for 1-2 h at room temperature. Alexa Fluor[®] 594 raised in
263 donkey anti-rabbit IgG (H+L) (Life Technologies) was used as secondary for both primary
264 antibodies, since they were used separately. Fluorescence images were captured on a Nikon
265 EC-1 confocal microscope using Nikon EZ-C1 software. The following laser/filter combinations
266 were used: DAPI nuclear stain (excitation 405 nm, emission BandPass 460/50 nm), eGFP
267 (excitation 488 nm, emission BandPass 509 nm) and Texas Red X Phalloidin (Invitrogen)
268 (excitation 543 nm, emission BandPass 605/70 nm).

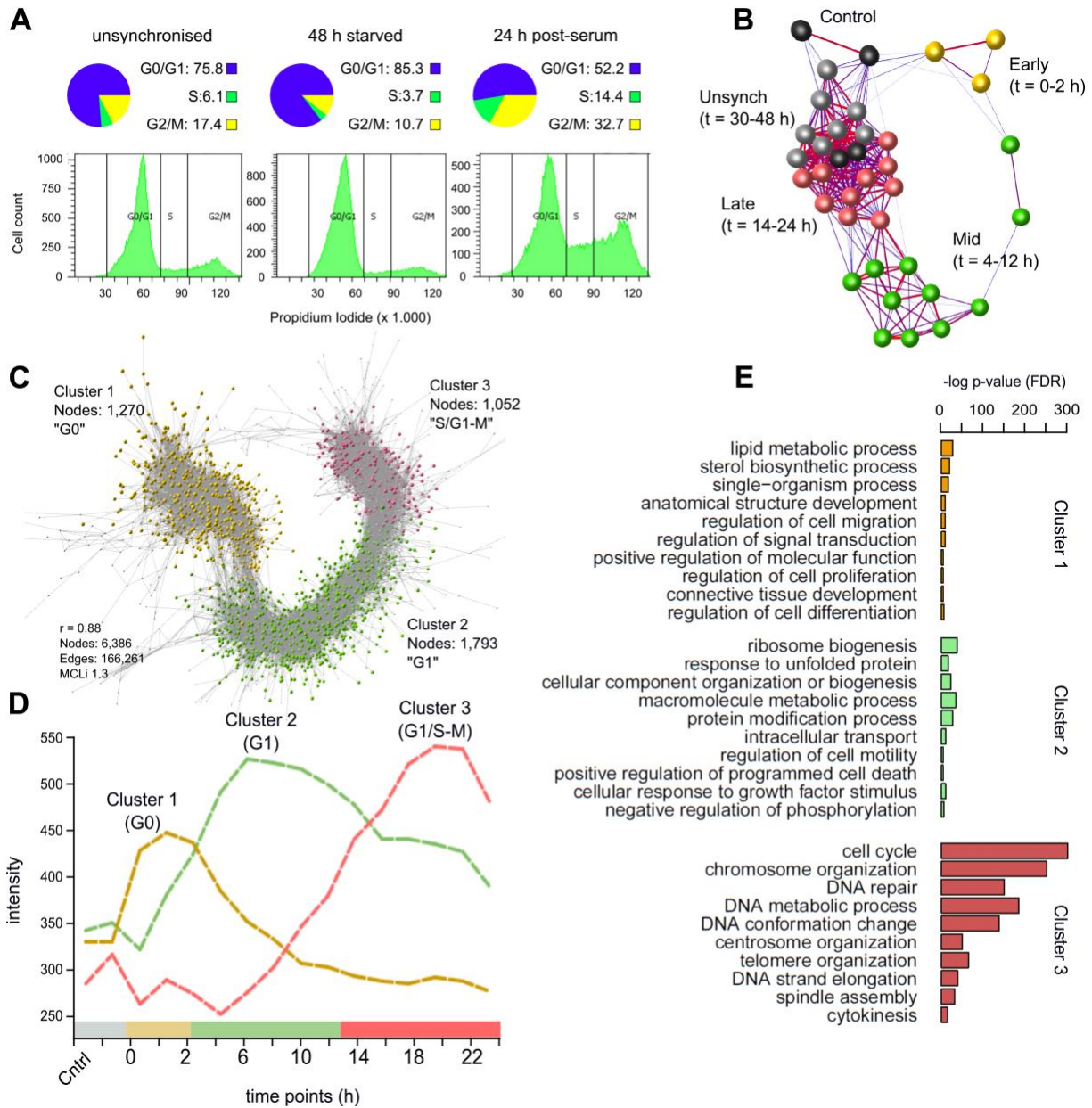
271 **Results**

273 **Identification of cell cycle-regulated genes in primary human fibroblasts**

274 Two time-course microarray experiments were performed on populations of normal human
275 dermal fibroblasts (NHDF) synchronised by serum starvation, as used previously for such
276 studies^{13,49}. Partial cell synchronisation was confirmed by flow cytometric analysis of

277 propidium iodide-stained cells. Following serum starvation approximately 40% fewer cells
278 were in the DNA replication phase (S) than in unsynchronised populations, and 24 h after the
279 re-addition of serum the number of cells undergoing division had increased by 3-4 fold (S and
280 G2/M phases) relative to the starved state (Fig 1A). Data derived from two transcriptomics
281 experiments, one monitoring the cells every 6 h for 48 h following release from starvation, the
282 second every 2 h over a period of 24 h, were subjected to quality control and corrected for
283 batch variation. The datasets were combined and analysed together using Graphia^{Pro}, a tool
284 designed to analyse numerical data matrices into correlation networks⁵⁰. A sample-to-sample
285 correlation network confirming the correspondence between the two experiments and time-
286 dependent transcriptional changes is shown in Fig 1B.

287
288 A gene-to-gene correlation network was then generated using a threshold of $r \geq 0.88$. This
289 value is well above the distribution of random correlations (S1A Fig) and set to minimise the
290 number of edges, while retaining a large number of nodes (S1B Fig). MCL clustering³³ of the
291 network was used to define the main phases of transcription associated with the cell cycle,
292 generating 23 gene clusters. The three largest clusters accounted for 96% of the genes
293 (probesets): NHDF_C1 (G0; 1,270 nodes, 1,176 unique Entrez IDs), NHDF_C2 (G1; 1,793 nodes,
294 1,739 unique IDs) and NHDF_C3 (S/G2-M; 1,052 nodes, 963 unique IDs) (Fig 1C). The average
295 gene expression profile of the three clusters over the first 24 h following the re-addition of
296 serum is shown in Fig 1D. NHDF_C1 comprised of genes induced during the starvation period
297 (0 h), but down-regulated soon after the re-addition of serum to the growth medium. The
298 average expression of genes within NHDF_C2 peaked around 6 h post-refeeding, consistent
299 with gap (growth) phase (G1)⁵¹. NHDF_C3 included genes which were induced between 12
300 and 20 h post re-feeding, many of which remained elevated in their expression at later time
301 points. Enrichment analysis performed on each gene cluster reported highly significant GO_BP
302 term enrichments for all three clusters, the most significant of which are shown in Fig 1E.
303 NHDF_C1 (G0-associated) was highly enriched with genes involved in lipid metabolism, such
304 as *lipid metabolic process* and *sterol biosynthetic process*, supporting the evidence that these
305 pathways are activated to adjust cellular metabolism during the starvation period⁵² (Fig 1E).
306 NHDF_C2 was enriched in biological processes associated with cell growth, such as *ribosome*
307 *biogenesis*, *macromolecule metabolic process*, *cellular component organisation* or *biogenesis*
308 *and intracellular transport* and included many of the known regulators of G1 including *E2F3*
309 and *CDK6*^{53,54}. Finally, NHDF_C3 was highly enriched with terms such as *chromosome*
310 *organisation*, *DNA repair*, *centrosome organisation*, *telomere organisation*, *DNA strand*
311 *elongation*, *spindle assembly* and *cytokinesis* (Fig 1E). Transcripts within this cluster plus all
312 nodes immediately adjacent to them (n+1), representing 1,207 unique Entrez IDs, were then
313 selected for further analysis. A more granular cluster analysis of this coexpression network
314 (MCLi 2.2) is presented in S1C Fig and S2 Table.



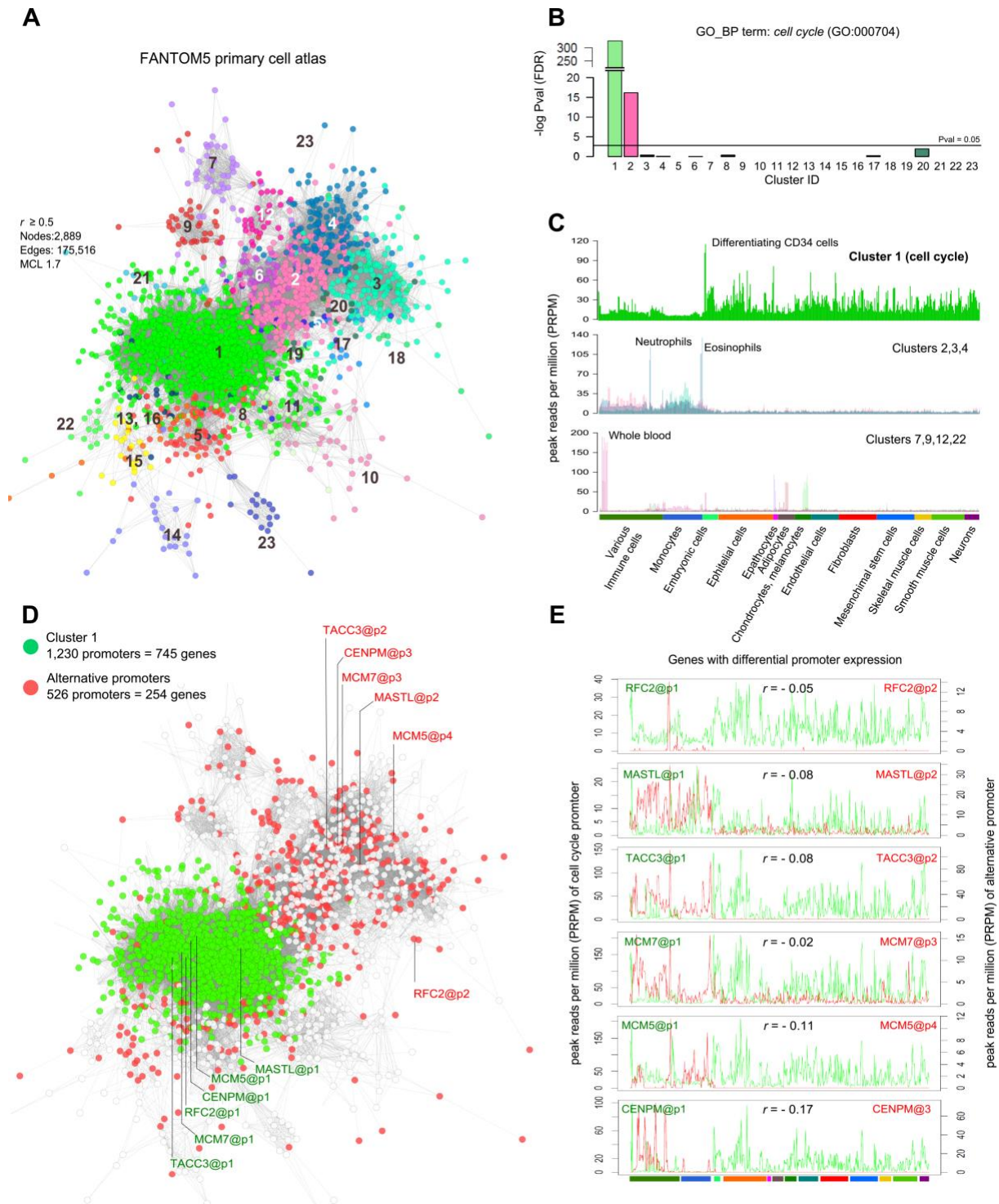
315
 316 **Fig 1. Network analysis of synchronised human fibroblasts (NHDF).** (A) Flow cytometry data monitoring
 317 fibroblasts entering proliferation after serum refeeding. In control samples 76% of cells are in G₀/G₁
 318 ("unsynchronised") but following 48 h of serum starvation the figure had increased to 85%, whilst the proportion
 319 of cells in S/G₂-M is decreased. 24 h post-serum 47% of cells were traversing S/G₂-M phase (over 3 times greater
 320 than starved populations). (B) Sample-to-sample correlation graph where nodes represent individual samples.
 321 Samples of starved cells (0 h) and early proliferative populations (1-12 h), form distinct sub-groupings in the
 322 network, with a clear progression from early to late time points. Synchrony is lost at later time points, and
 323 samples group with unsynchronised populations. (C) Correlation graph of the transcriptional network of
 324 synchronised fibroblasts from a quiescence through to mitosis. The graph divides in three large clusters:
 325 NHDF_C1 (yellow) corresponds to genes whose expression is greatest in quiescent fibroblasts and decreases
 326 during the entry into mitosis (G₀); NHDF_C2 genes (green) expression is associated with G₁, their expression
 327 peaking between 1 and 8 h after the addition of serum; and the expression of genes in NHDF_C3 (red) start to
 328 rise from the beginning of the G₁/S transition to mitosis. Nodes represent individual probesets. (D)
 329 Corresponding average expression profiles of genes in NHDF_C1-3. (E) GO enrichment analysis on the gene
 330 content of the three clusters.

331
 332

333 **Refinement of the core cell cycle gene signature**

334 To refine the candidate list of NHDF S/G2-M phase-associated genes and eliminate genes that
335 may be specific to differentiated fibroblast function, we examined their expression using the
336 FANTOM5 consortium promoter level CAGE data (HCF5), derived from more than 100
337 different primary human cell types (495 samples)²⁷. The 1,207 genes identified in the NHDF
338 data were mapped to the FANTOM5 dataset returning 3,145 promoters with expression >5
339 TPM (tags per million) in at least one sample. These data were subjected to network analysis
340 ($r \geq 0.5$). The graph contained 2,889 promoters (nodes) and 175,516 edges from which the MCL
341 cluster algorithm (MCLi = 1.7) also generated 23 clusters (Fig 2A). HCF5_C1 (1,230 promoters
342 of 745 genes) was enriched for cell cycle-associated genes (Fig 2B). Of the others, only
343 HCF5_C2 exhibited any enrichment for the GO_BP term 'cell cycle' but at a much lower
344 significance (Fig 2B). The average expression of HCF5_C1 gene promoters was greatest in
345 highly proliferative cell populations such as embryonic stem cells, epithelial cells and a
346 population of CD34⁺ hematopoietic stem cells. In contrast, monocytes displayed minimal
347 expression of these genes, reflecting the low rate of proliferation in these populations⁵⁵ (Fig
348 2C, top profile). The remaining HCF5 clusters contained promoters with a diverse range of
349 expression profiles (Fig 2C). Many genes within HCF5_C1 also included alternative promoters
350 (254 genes, 526 promoters) with distinct expression profiles that clustered independently (Fig
351 2D). Highlighted are six genes with known functions in the cell cycle, three of which, *RFC2*,
352 *MCM5* and *MCM7* encode proteins known to be required for DNA replication⁵⁶. The
353 alternative promoters were most highly-expressed in immune cell types (Fig 2E).

354
355 Based upon the merge of the two datasets, the initial list of 963 genes (1052 probesets)
356 generated from the analysis of NHDF cells, was reduced to a list of 745 genes with promoters
357 in HCF5_C1 from the FANTOM5 data where the expression was tightly correlated across
358 diverse human cell populations.



359
360
361
362
363
364
365
366
367
368
369
370

Fig 2. Co-expression of promoters associated with S/G2-M fibroblast genes across the FANTOM5 primary cell atlas. (A) Clustered graph representing the promoters of the S/G2-M phase associated genes identified in the NHDF data and their correlated expression in the context of the FANTOM5 primary cell atlas. Nodes represent individual promoters, their colour representing membership to co-expression clusters. **(B)** GO enrichment analysis for the GO_BP term *cell cycle* on each of the 23 clusters identified, cluster 1 to be highly enriched in cell cycle genes. **(C)** The expression profile of the HCF5_C1 promoters showed them to be transcribed in a wide variety of primary cells with highest expression in embryonic cells and a number of epithelial cells, but a relatively low expression in monocytes (top). In contrast other clusters, not enriched in cell cycle gene promoters, exhibited a different pattern of expression. The average expression of clusters HCF5_C2, 3 and 4 promoters was greatest in immune cell populations (middle). Others (bottom) exhibited cell type-specific expression, e.g. hepatocytes (HCF5_C7), adipocytes (HCF5_C9), whole blood (HCF5_C12) and melanocytes (HCF5_C22). **(D)** Nodes in the graph

371 shown in A, were color-coded to show differential promoter expression. HCF5_C1 (green nodes) is comprised of
372 1,230 promoters corresponding to 745 genes, the red nodes represent an additional 526 promoters associated
373 with 254 of the HCF5_C1 genes. (E) Promoter expression profiles of six genes being driven by promoters
374 associated with the cell cycle (green profile) and expression of their alternative promoters (red profile).

375

376 **Manual curation of the S/G2-M cell cycle list**

377 The 745 genes identified above were individually curated. We removed 198 genes that were
378 induced late in G1 and in advance of the likely onset of S phase. Conversely, we restored 132
379 genes, where the literature or other data (see below) indicated that they function in the cell
380 cycle and individual examination of the FANTOM5 data indicated that they were, indeed,
381 relatively more highly-expressed in proliferating cells, albeit not included in HCF5_C1.

382

383 To examine the inter-species conservation of the S/G-M transcriptional network, an additional
384 transcriptomics experiment was performed on synchronised mouse embryonic fibroblasts
385 (MEF). The majority of mouse/human orthologues showed a conserved expression pattern
386 across the cell cycle (Fig 3A). The transcriptional network of the mouse fibroblast data was
387 similar in topology to the NHDF data (S2A-B Fig) and an additional 22 known cell cycle genes
388 were observed to co-cluster with the S/G2-M phase genes in these cells.

389

390 The merged outcomes of the comparative analysis and manual curation of these data
391 produced a set of 701 cell cycle regulated genes (see S2 Fig and S2 Table for a detailed cluster
392 analysis of these data). The genes were then assigned to either 'S' or 'G2-M' phases by
393 correlating them with the expression of known cell cycle phase-specific factors: *CDC25A* and
394 *BRCA1* (S phase), and *CDK1* and *CCNB1* (G2-M phase)⁵⁷⁻⁵⁹. Accordingly, 380 genes were
395 assigned to S phase and 321 to G2-M phase (S3A Fig). The two sets of phase-associated genes
396 were analysed for enrichment of known binding motifs. Both sets were significantly enriched
397 with cell cycle transcription factor binding sites. Amongst others S phase genes were shown
398 to be highly enriched for E2F sites (10^{-59}) and the G2-M genes for CHR (10^{-15}) and NFY (10^{-24})
399 sites (for detailed results see S3B Fig). Phase annotation was also consistent overall with those
400 of previous cell cycle studies (S3C Fig).

401

402 After a systematic database and literature-based curation of the gene list, the majority (496)
403 were found to be functionally associated with a cell cycle-related process (Fig 3Bi). For
404 example, *DNA damage* and *DNA replication* linked predominantly with S phase annotated
405 genes, and *Chromosome partition* and *Spindle assembly and regulation* being associated
406 mainly with G2-M phase (Fig 3Bii). Other categories included a similar number of genes
407 induced at either phase, such as *Cell cycle regulation*. For 205 genes little or no direct evidence
408 of a direct involvement in the cell cycle could be found, although in some cases there was
409 circumstantial evidence to support this relationship, e.g. publications showing their
410 expression to be elevated in cancer. These genes are classified as 'putative' cell cycle genes.
411 Others in this category encode proteins that function within pathways that potentially relate
412 to cell division, e.g. apoptosis, whilst the association of yet others would appear more

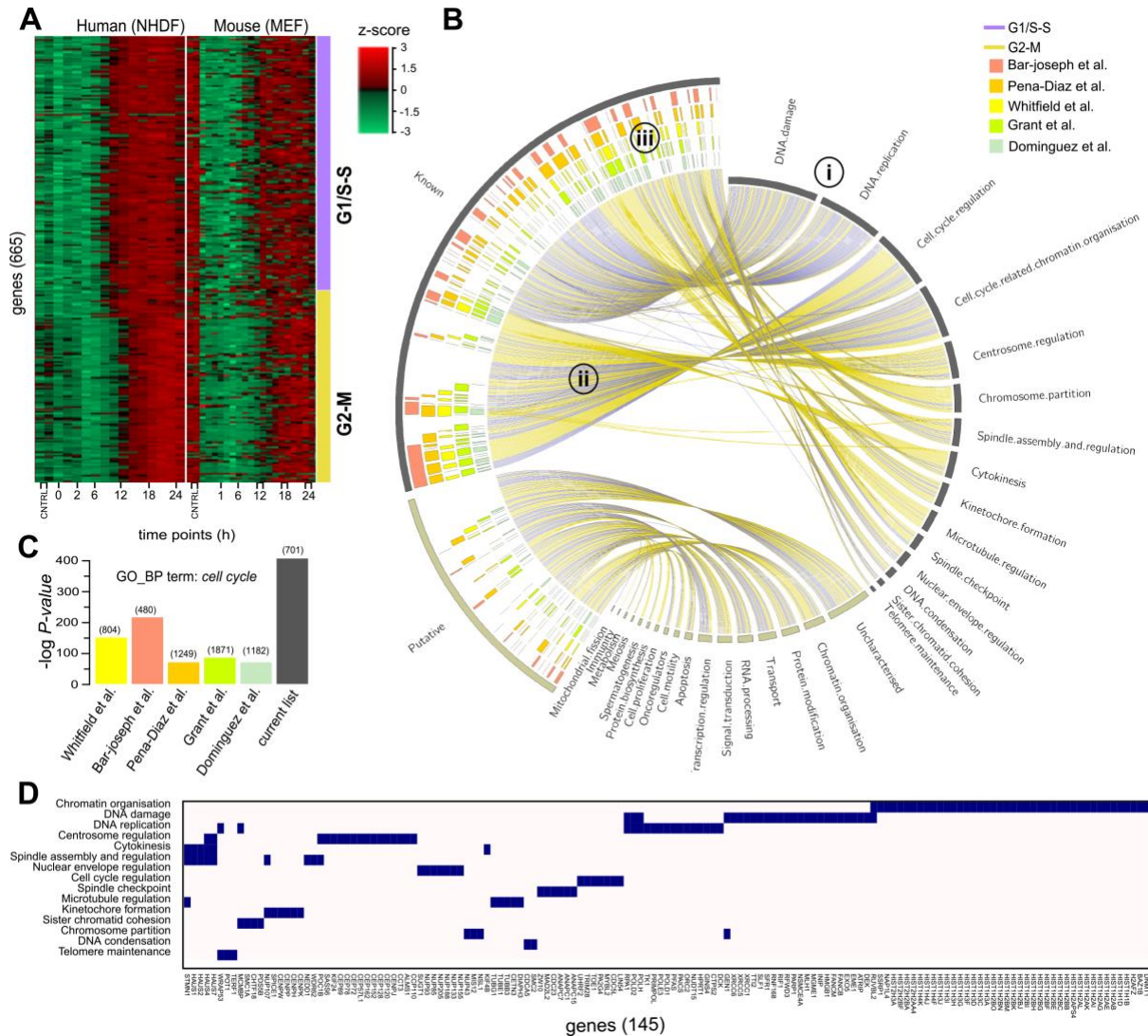
413 tenuous, e.g. RNA processing and immunity. For 53 genes, no functional information was
414 found.

415

416 There is a significant overlap between our S/G2-M gene list and the cell cycle gene lists
417 generated by previous studies (Fig 3Biii). However, the current list showed a greater
418 enrichment of genes with the GO_BP term *cell cycle* when compared with published cell cycle
419 lists (Fig 3C). Indeed, many well-validated S/G2-M phase genes (145) were not shown to be
420 regulated in any of the previous transcriptomics study, including mitotic regulators such as
421 *MADL2L2*, four members of the augmin complex *HAUS1,2,4,7*, three members of the APC/C
422 cyclosome complex, *ANAPC1,7,15*, multiple DNA replication-dependent histone isoforms (36)
423 and several genes encoding components of the centrosome (*CEPs*) and the nucleopore
424 complex (*NUPs*) (Fig 3D). Conversely, there were 345 genes annotated with the GO_BP term
425 *cell cycle* identified by at least one of the five previous human transcriptomics studies but not
426 the current study. When examined in the context of the current NHDF data, many were
427 induced during G1, whereas others did not show significant variation in their expression over
428 the cell cycle (S4 Fig). As noted above, we have deliberately excluded genes that are known
429 to be induced in G1, although this gene set may include genes that are essential for cell cycle
430 progression²⁶.

431

432 A table of all 701 genes, which includes eight pseudogenes and three non-coding RNAs, with
433 corresponding classifications and evidence supporting their functional association with cell
434 cycle can be found in S1 Table. A simple confidence score was calculated for all genes in the
435 list based on available experimental evidence from this and previous studies.



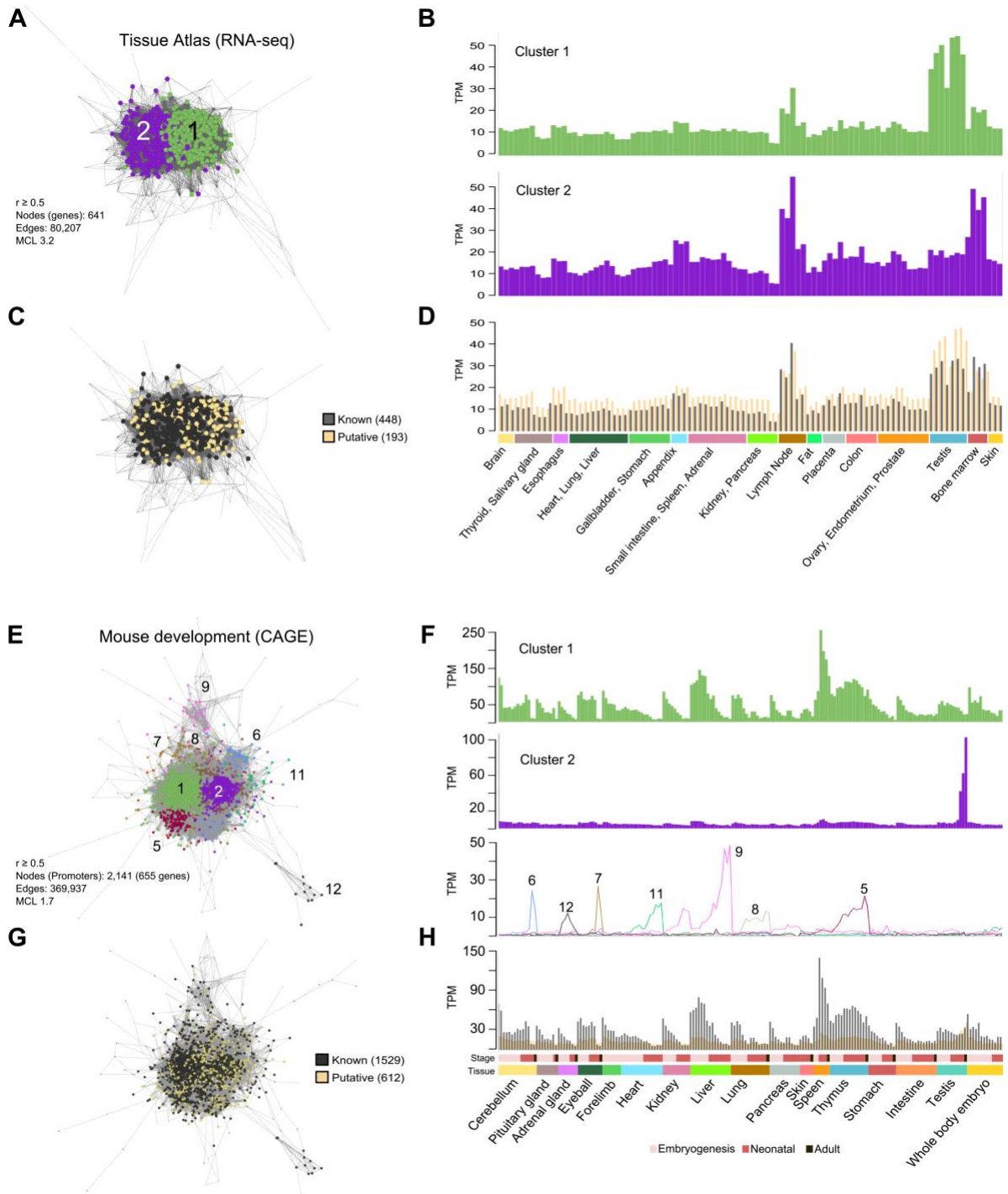
436
437
438
439
440
441
442
443
444
445
446
447
448

Fig 3. Analysis of the S/G2-M transcriptional network. (A) Heatmaps demonstrate a highly conserved pattern of expression between human S/G2-M phase associated genes and their 667 mouse orthologues over the first 24 h in human fibroblasts (NHDF) and mouse embryonic fibroblasts (MEF) following serum refeeding. Genes were ordered by the phase assignment calculated from the NHDF data. (B) CIRCOS plot showing the associations between the 701 S/G2-M human genes identified here and (i) the functional category with which they have been manually curated to belong. They have been divided as the whether they are 'known' or 'putative' cell cycle genes. (ii) Edges are coloured based on the phase assigned from the NHDF data. (iii) The inner coloured blocks show genes reported by previous human cell cycle transcriptomics studies. (C) Histogram of GO enrichment scores for the GO_BP term *cell cycle* for the current and previously published cell cycle lists. (D) Block diagram showing the functional category assignment of the 145 genes reported in the literature to be cell cycle-associated, but undetected by previous transcriptomics cell cycle studies.

Validation of the S/G2M transcriptional network using independent data

To further validate the conservation of co-expression of the S/G2-M gene list, we explored two additional datasets. The first was a human tissue expression atlas (HTA) of RNA-seq data derived from 95 samples of 27 human tissues³². Of the 701 S/G2-M genes defined here, 655 were identified in these data and their co-expression examined. At a correlation of $r \geq 0.5$, 641 genes were present in the graph, which divided into two MCL-defined clusters encompassing 549 genes (Fig 4A). The genes in these clusters were expressed widely, with an elevated expression level associated with proliferative tissues (Fig 4B). HTA_C1 was comprised of genes

457 whose expression in the testis was higher (Fig 4B, top) as compared to the expression of
458 HTA_C2 genes, which showed highest expression in bone marrow and lymph node (Fig 4B,
459 bottom). The majority of known S/G2-M genes clustered together and significantly, so did the
460 putative cell cycle genes (Fig 4C-D), supporting their association with this system. A second
461 promoter-level dataset produced by the FANTOM consortium (MDF5)²⁷, comprised of 17
462 mouse tissues sampled at multiple intervals during embryogenesis and post-neonatal
463 development. Again the data for only the S/G2M genes (2,141 promoters mapping to 658
464 genes) was examined. Similarly, the majority of the promoters/genes co-clustered, with the
465 exception of a few small clusters (Fig 4D). In general the promoters in MDF5_C1 exhibited
466 highest expression in embryonic tissues, their expression markedly decreasing with
467 developmental age, a pattern reflecting the reducing rate of proliferation during development
468 (Fig 4F, top profile). A notable exception to this was in the case of the spleen and thymus,
469 where expression peaked around birth. In line with observations in the human tissue atlas
470 dataset, a portion of S/G2-M genes (MDF5_C2) were predominately expressed in adult testis
471 (Fig 4F, middle profile). Multiple smaller clusters, the majority of which were associated with
472 alternative promoters of cell cycle-associated genes, exhibited tissue-specific promoter
473 expression (Fig 4F, bottom profile). Again putative S/G2M genes were co-expressed with the
474 known cell cycle genes (Fig 4G-H). Co-expression of the S/G2-M genes within the context of
475 all genes are shown in S5A-B Fig, for the HTA dataset and in S5C-D Fig for the MDF5 dataset.
476 Promoter analysis of the 205 putative cell cycle genes alone showed that they were enriched
477 in known S/G2-M transcription factor binding sites, i.e. for E2Fs and NFY, further supporting
478 their associated with cell division (S5E Fig).



479
 480 **Fig 4. Confirmation of coexpression of S/G2-M genes across human and mouse tissues. (A)** Clustered
 481 coexpression network of S/G2-M genes across human tissue atlas (HTA). **(B)** The average expression profile of
 482 the genes in the two main clusters is very similar with the exception that genes in HTA_C1 are strongly expressed
 483 in the testis. **(C)** Interesting both known and putative cell cycle genes cluster together, **(D)** having very similar
 484 expression profiles. **(D)** Clustered coexpression network of promoter level data of mouse orthologues of human
 485 S/G2-M genes in the mouse development dataset from FANTOM5 (MDF5). Here a number of clusters are
 486 observed. **(F)** The largest group (MDF5_C1) are highly expressed in all developing tissues but expression levels
 487 generally decrease with age. However, in the case of spleen and thymus highest levels of express are observed
 488 around birth. MDF5_C2 promoters are highly expressed in adult testis and alternative promoters that form the
 489 majority of other clusters show a variety of tissue-specific expression patterns. **(G-H)** Promoters for known and
 490 putative cell cycle genes cluster together and exhibit a similar expression profile.

491

492

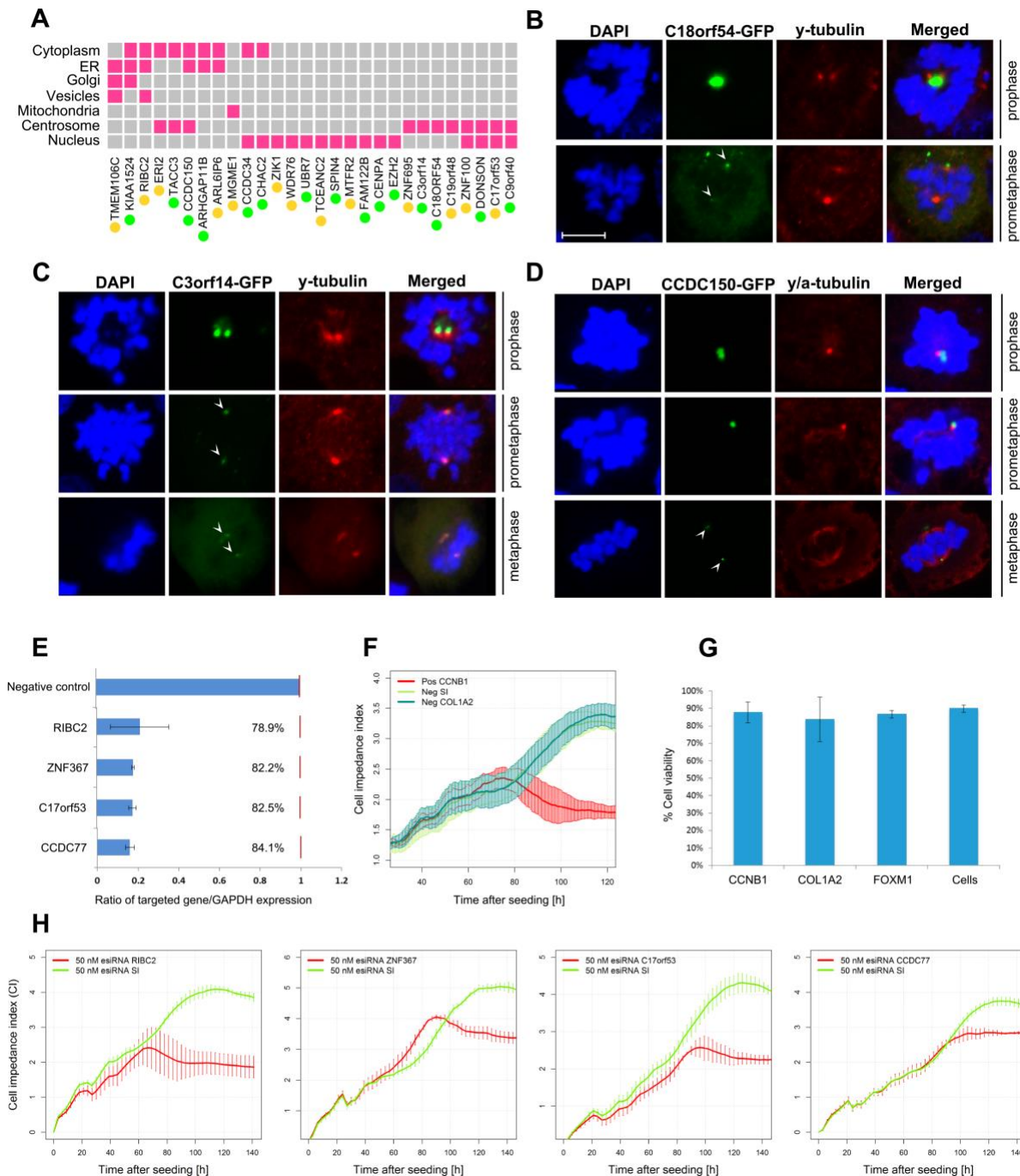
493 **Experimental corroboration of the uncharacterised S/G2-M genes**

494 Many gene products required for S/G2-M phase, are localised to specialised cell cycle-
495 associated organelles or structures. For example, chromosome segregation during mitosis
496 requires formation of kinetochores at centromeres and the correct attachment of
497 kinetochores to spindle microtubules emanating from microtubule organising centres, e.g.
498 centrioles and centrosomes. Accordingly, we tested the subcellular localisation of 28
499 candidate genes by cDNA transfection in HEK293 cells. As positive controls we included
500 CENPA, TACC3, DONSON and MGME1⁶⁰⁻⁶³, the localisation of which were confirmed by these
501 assays (S1 Data). Each ORF was tagged with GFP at both the C- and N-terminals^{48,64}. After
502 inspection of the expression of the 56 protein constructs (two per clone), their subcellular
503 localisation was analysed (S2 Data). As summarised in Fig 5A, nuclear localisation was the most
504 frequently observed (15/28) followed by centrosomal-like localisation (11/28) and cytosol
505 (9/28). In some instances localisations were congruent with organelles such as the ER, Golgi
506 apparatus, vesicles and mitochondria, possibly representing non-specific protein deposits. In
507 around half of cases, the C- and N-terminal tagged proteins produced the same localisation
508 (Fig 5A). No cases of completely discrepant localisations between the two constructs were
509 observed. For the 11 constructs showing centrosomal-like staining, we examined their
510 expression along with centrosomal marker γ -tubulin. Of these, C18orf54, C3orf14 and
511 CCDC150 clearly co-localised with γ -tubulin during different mitotic stages, i.e. prophase,
512 prometaphase and metaphase (Fig 5B-D). For the other constructs co-localisation with γ -
513 tubulin was not demonstrated (not shown). Confocal images of all 28 proteins screened can
514 be found in S1 Data.

515

516 To examine whether reducing the expression of the novel S/G2-M phase genes affected cell
517 proliferation, we tested the effect of mRNA knockdown in human fibroblasts using esiRNAs.
518 We achieved around 80% knock-down efficiency in all cases examined (Fig 5E). As a positive
519 control, knockdown of cyclin B1 (*CCNB1*) produced a strong inhibition of cell proliferation
520 compared to control esiRNAs (Fig 5F) and transfection had no effect on cell viability (Fig 5G).
521 Of the 39 knockdowns of known cell cycle-regulated genes tested, only twelve (*ARHGAP11A*,
522 *CCNB1*, *CCNE1*, *CENPA*, *CEP85*, *ESPL1*, *FAM111A*, *FIGNL1*, *FOXM1*, *KIF11*, *MAD2L1*, *REEP4*) had
523 a significant impact on the rate of cell proliferation. Similarly, of the 22 uncharacterised cell
524 cycle genes 10 (*C17orf53*, *CCDC77*, *DEPDC1B*, *FAM72B*, *GSTCD*, *NEMP1*, *RIBC2*, *RPL39L*, *UBR7*,
525 *ZNF367*) significantly inhibited proliferation (Fig 5E; results of these analyses in S2 Data). The
526 Mitocheck database is a resource listing the cellular phenotypes from a genome-wide RNAi-
527 screen of human proteins, recorded by high-throughput live cell imaging⁸. Of the known gene
528 components listed for which results were available, 136/490 (27.8%) resulted in one or
529 multiple cell phenotypes pointing to cell cycle defects. Amongst the candidate cell cycle genes,
530 12.8% were associated with a cell cycle phenotype. For example, *ZNF85* silencing led to
531 abnormal chromosome segregation and mitotic metaphase plate congression, knock-down of
532 *ZNF90*, *UBALD2* and *CCDC34* led to cell death and *ZNF738*, *CCDC150* and *ZNF788* knockdowns

533 resulted in abnormalities in the size and shape of nuclei. Mitochek results have been added
 534 to the gene list presented in S1 Table. Finally, ToppGene⁶⁵ was used to search for phenotypes
 535 significantly associated with mutations in the S/G2-M genes. In man, 79 phenotypes were
 536 identified, the most significant of which included embryonic growth defects, e.g.
 537 microcephaly, growth retardation and various cancers. In mouse, 242 phenotypes were
 538 recorded as enriched, the most significant were abnormal cell cycle, embryonic lethality and
 539 abnormal nuclear morphology, again supporting a strong association with cell cycle defects. A
 540 full list of the phenotypes enriched for this list and the genes associated with them is provided
 541 in S3 Table.



542 **Fig 5. Subcellular localisation and RNAi assays of candidate cell cycle components.** (A) Matrix summarising the
 543 subcellular localisations of the 28 proteins screened. For a full description of these data see S1 Data. (B-D)
 544 C3orf14, CCDC150 and C18orf54 were found localised on the centrosomes at different stages of mitosis. Proteins
 545

546 are tagged with GFP (green), nuclei are stained with DAPI (blue), and centrosomes marked with anti γ -tubulin
547 antibody (red). Scale bar = 10 μ m. **(E)** Knock-down efficiencies of siRNA against four potential novel cell cycle
548 genes measured as the ratio between the silenced gene expression and GAPDH expression. **(F)** Positive control
549 cyclin B (*CCNB1*) silencing decreased cell impedance index (proliferation) compared to negative controls for
550 sucrase-isomaltase (*SI*) and collagen 1 A2 (*COL1A2*). **(G)** Viability assays after gene knock-down of two known cell
551 cycle regulators (*CCNB1* and *FOXM1*) and a negative control (*COL1A2*) compared to untransfected cells. **(H)**
552 Proliferation profiles following gene knock-down of four uncharacterised but putative cell cycle genes *RIBC2*,
553 *ZNF367*, *C17orf53* and *CCDC77* compared to knock down of *SI*. For a full description of the results all knock-down
554 experiments performed here, see S2 Data.

555

556 Discussion

557 Mitotic cell division is perhaps the most fundamental of all biological processes and functional
558 orthologues of many of the core components are conserved across species. Curated databases
559 list and classify the function of cell cycle components⁶⁶ and place them into pathways^{39,67}. In
560 every system studied, from yeast to man, there are numerous genes required for cell division
561 that are transcriptionally regulated and associated with a given phase of the cell cycle^{17,68}. It
562 could be argued that all genes involved in anabolic processes are cell cycle-related, since an
563 increase in cell size is usually precondition for cell division. Similarly, genes regulating entry
564 into the cycle, e.g. growth factors, are often considered to be cell cycle proteins. In the context
565 of this work, we use the term to refer only to the set of proteins that are required when a cell
566 commits to undergo mitosis²⁰. Accordingly, we have sought to define the core set of cell cycle
567 genes expressed during mammalian S/G2-M, demonstrating them to form a highly correlated
568 transcriptional network across tissues and cell types. As a gene signature, S/G2-M genes
569 effectively define the mitotic index of a cell population.

570

571 The gene expression patterns observed here in fibroblasts were broadly consistent with
572 previous studies using the same cell type and synchronisation method^{13,49}. However, a wound-
573 healing response, triggered by the serum, may confuse efforts to identify cell cycle-related
574 transcripts in fibroblasts¹⁸. To circumvent this issue, we complemented our analysis by
575 examining the co-expression of the fibroblast-derived S/G2-M associated genes using the
576 FANTOM5 primary cell atlas²⁷ to remove genes that showed evidence of cell-specificity in their
577 expression. These analyses were further refined by comparison to expression studies in
578 synchronised mouse fibroblasts and detailed examination of the primary data. The result is a
579 list of 701 S/G2-M-regulated genes, which are highly enriched in relevant GO terms and
580 transcription factor binding sites. Based on manual curation of published reports, 496 of these
581 genes encode 'known' cell cycle proteins, many listed as such in annotation databases e.g. GO
582 and UniProtKB. This list partially overlaps with the findings of previous transcriptomics studies
583 on human cells but interestingly, transcriptional regulation of 145 of the known S/G2-M
584 associated genes was not detected in any of the earlier reports^{13-16,18}. The majority of previous
585 studies sought to define cell cycle genes as having a wave-like expression profile over multiple
586 rounds of cell division, using Fourier transform-based methods to identify them. However, cell
587 division in populations of cells rapidly becomes asynchronous, and a fraction of them do not
588 commit to a second cycle¹³. In the current study, this fact was reflected in the loss of
589 synchrony in the cell cycle gene expression signature after 30 hours, consistent with FACS

590 analyses (data not shown). Not only did previous studies exclude many bona fide cell cycle
591 genes the different criteria and analytical methods used produced a poor consensus¹⁵. The
592 correlation-based network approach used in this study is a more efficient way to identify
593 phase-specific cell cycle genes²⁰.

594

595 The strong association of the many putative cell cycle genes identified here was further
596 demonstrated by their conserved coexpression across adult human and developing mouse
597 tissues. Some of the S/G2-M phase genes we identified have only been validated relatively
598 recently. For example, *PRR11* (proline rich 11), mutations in which have been associated with
599 cancer, was shown to regulate S to G2-M phase transition⁶⁹. Links to cancer biology also
600 suggests function for two of the three lncRNAs identified by this study, *DLEU1&2*^{70,71}. There
601 are nine genes annotated as being involved in apoptosis, a process that can be initiated if a
602 cell fails a mitotic check point. *CASP2*, long considered to be an orphan caspase⁷², is recognised
603 as a key factor in driving cell apoptosis (mitotic catastrophe) triggered by mitotic
604 abnormalities, such as defects in chromosomes, mitotic spindles, or the cytokinesis
605 apparatus^{73,74}. Other genes within the list await functional validation.

606

607 Amongst the 205 putative cell cycle genes, there are 53 complete functional orphans.
608 Fourteen of the 27 we tested localised wholly or partially to the nucleus and 11 showed
609 evidence of centrosomal localisation, an organelle vital for cell cycle progression⁷⁵. Another
610 three, *CCDC150*, *C3orf14* and *C18orf54* co-localised with γ -tubulin (a centrosomal marker). A
611 recent study confirmed this localisation for *C3orf14*⁷⁶. The sub-cellular localisations reported
612 here were in many cases also supported by IHC results reported by the Human Protein Atlas
613 database^{37,37} (data not shown). RNAi knockdown assays were also performed on a range of
614 known and uncharacterised genes from the list. In these assays, 10 of the 22 uncharacterised
615 proteins showed differences in the rate of cell proliferation following gene knockdown,
616 suggesting non-redundant functions in cell proliferation, with a hit rate slightly higher than
617 the known cell cycle genes tested (Fig 5H). Taken together, these validation data suggest that
618 the large majority of the novel cell-cycle regulated genes identified here will be found to
619 function in some aspect of S/G2-M biology.

620

621 The FANTOM5 human and mouse promoterome data provide definitive locations for the
622 transcription start sites of genes. Of the 701 genes identified here, in the primary cell atlas
623 data at least 254 use alternative promoters that drive their expression outside of the context
624 of the cell cycle. Among them, three are involved in the assembly of the replisome, namely:
625 *MCM5*, *MCM7* and *RFC2*⁵⁶, and had significant expression from alternative promoters in
626 certain immune-related cell populations. This observation is in accordance with a previous
627 report showing that factors of the minichromosome maintenance complex (MCMs), including
628 *MCM5* and *MCM7*, were found to be present on the *IRF1* promoter in *STAT1*-mediated
629 transcriptional activation, when cells were treated with *IFN- γ* ⁷⁷. *MCM5*, in particular, was
630 shown to directly interact with *STAT1* and to be necessary for transcriptional activation⁷⁸.
631 Similar observations were made in the analysis of the mouse development time course data,

632 where many bona fide cell cycle proteins are strongly expressed in the testis, where they may
633 play a role in meiosis or be part of the centrosomal biology associated with flagella. The
634 'moonlighting' of cell cycle genes in other scenarios also likely breaks up the transcriptional
635 signature in co-expression analyses across datasets comparing tissues or cells²¹⁻²⁵. These
636 alternative transcripts may be regulated in a unique manner to support DNA-dependent
637 processes such as recombination, somatic hypermutation and class switching that are unique
638 to leukocytes, or other distinct functions.

639

640 In summary, this study set out to define the transcriptional network associated with the final
641 stages of the human cell cycle, between entry into S phase through to the completion of
642 mitosis. The aim was not only to summarise the known components of this system but to
643 identify new ones. Through detailed analyses of multiple human and mouse datasets we have
644 defined 701 genes as being upregulated during the S/G2-M phase of the cell cycle, many of
645 which are conserved across species. Based on promoter expression some proteins would
646 appear to function exclusively within the context of cell division, others would appear to have
647 additional roles outside of this system. Functional assays performed on a number of the
648 uncharacterised genes strongly suggests that many are indeed novel components of the cell
649 cycle machinery. The gene list provided represents the first comprehensive list of
650 experimentally derived and validated S/G2-M phase associated genes. As such this work
651 provides a valuable resource of both the known and potentially novel components that make
652 up the many pathways and processes associated with mitotic cell division.

653

654 **Supplementary Captions**

655

656 **S Fig1. Analysis of NHDF transcriptomics data. (A)** Plot shows the distribution of correlation
657 values between 2,000 genes randomly selected from the NHDF data compared with that of
658 the same genes but with permuted values. The threshold used for analysis excludes random
659 correlations. **(B)** Plot showing number of edges and nodes as a function of the correlation
660 coefficient. A threshold of $r \geq 0.88$ was selected to include a minimal number of edges, while
661 retaining a large number of nodes. **(C)** Network graph of the data clustered at MCLi 2.2 and
662 average expression profiles of the main clusters showing gene expression as a function of
663 time.

664

665 **S Fig2. Network analysis of the MEF data. (A)** Network graph of the MEF data (MCLi 2.2) at r
666 ≥ 0.88 . **(B)** Average expression profile of the major clusters of cell cycle related genes.

667

668 **S Fig3. Phase assignation analysis and comparison with previous data. (A)** The 701 genes
669 associated with S/G2-M phase were assigned as being either 'S' or 'G2-M' phase according to
670 their correlation with *bona fide* phase-specific cell cycle genes (see text), resulting in 380 S
671 phase genes and 321 G2-M genes. **(B)** Motif enrichment analysis performed using HOMER
672 were run on the two gene subsets returning significant enrichments for motifs bound by
673 transcription factors known to be active in the corresponding phases. **(C)** Our phase

674 assignment was compared to those of five previous studies. Heatmaps for each of these
675 comparisons show overall consistent phase assignment.

676

677 **S Fig4. Expression of the 701 S/G2-M genes identified here and 345 other cell cycle-**
678 **annotated genes.** Expression of the 701 genes show up-regulation associated with entry into
679 S phase through to the completion of M phase. The majority of the other 345 genes identified
680 by the five previous cell cycle studies^{13,14,18,34,35} but not in this study and associated with the
681 GO_BP term cell cycle showed induction at earlier time-points. Expression values were
682 transformed to z-score (see legend).

683

684 **S Fig5. Coexpression networks of human tissue (HTA) and mouse tissue development**
685 **(MDF5). (A)** Clustered coexpression network of HTA analysis, showing clusters of genes
686 exhibiting specific expression patterns. The location of the majority of cell cycle genes is
687 highlighted by dotted red lines and in this graph reside in cluster HTA_C6. **(B)** Enrichment
688 analysis shows this cluster to be highly enriched in genes with the GO_BP term cell cycle and
689 with genes included in our list. **(C)** Clustered coexpression network of MDF5 analysis, showing
690 clusters of genes exhibiting specific expression patterns. Cell cycle genes clusters are
691 highlighted by dotted red lines. **(D)** Enrichment analysis shows clusters MDF5_C11, MDF5_C27
692 and MDF5_C1 to be significantly enriched with the GO_BP term *cell cycle* and with genes
693 included in our list. **(E)** Motifs enrichments of ten randomly selected subsets of the known
694 group of S/G2-M genes (left) equivalent to the number of putative S/G2-M genes (right).
695 Significant cell cycle-associated TF, such as E2Fs and NFY, were identified in both cases.

696

697 **S Table 1. List of all known and putative S/G2-M phase associated genes identified by the**
698 **current study.** The table contains an annotated list of 701 genes identified by this study and
699 the evidence from the current and previous studies linking them to the cell cycle.

700

701 **S Table 2. Clustering results from network analysis of the NHDF and MEF cell cycle associated**
702 **transcriptome.** Lists of genes whose expression is regulated at any point during the cell cycle
703 in human and mouse of mouse fibroblasts.

704

705 **S Table 3. Phenotypes associated with mutations in S/G2-M phase genes.** ToppGene was
706 used to analyse what human and mouse phenotypes are associated with the 701 genes
707 identified here and statistically over-represented. This table provides a full list of these
708 phenotypes and which genes they are associated with.

709

710 **S Data 1. Results from subcellular localisation studies of uncharacterised cell cycle proteins.**
711 A summary of results from experiments using GFP-tagged proteins to study the localisation of
712 a number of uncharacterised putative cell cycle proteins.

713

714 **S Data 2. Results of RNAi screens of uncharacterised cell cycle proteins.** A summary of the
715 results from esiRNA knockdown studies of known and putative cell cycle genes.

716

717

718 **Acknowledgement:** B.G. is a recipient of a BBSRC funded EastBio studentship. T.L. is
719 supported by a Sir Henry Dale Fellowship jointly funded by the Wellcome Trust and the Royal
720 Society (206211/Z/17/Z). The Wellcome Centre for Cell Biology is funded by Wellcome grant
721 203149/Z/16/Z. M.B., D.A.H. and T.C.F. are funded by an Institute Strategic Grant from the
722 Biotechnology and Biological Sciences Research Council (BBSRC) (BB/JO1446X/1).

723

724 **Author contributions:** B.G., M.B., T.R. and S-H.C. performed the majority of laboratory work
725 described here. B.G. and T.C.F. performed the bioinformatics analyses and, B.G., T.L., S.W.,
726 D.A.H. and T.C.F. wrote and edited the manuscript. T.C.F. supervised the project and
727 conceived of the idea behind the work.

728

729 **Competing interests:** The authors have no conflict of interest.

730

731

732 **References**

- 733 1 Vermeulen, K., Van Bockstaele, D. R. & Berneman, Z. N. The cell cycle: a review of
734 regulation, deregulation and therapeutic targets in cancer. *Cell Prolif* **36**, 131-149
735 (2003).
- 736 2 Delaval, B. & Birnbaum, D. A cell cycle hypothesis of cooperative oncogenesis
737 (Review). *Int J Oncol* **30**, 1051-1058 (2007).
- 738 3 Wiman, K. G. & Zhivotovsky, B. Understanding cell cycle and cell death regulation
739 provides novel weapons against human diseases. *J Intern Med* **281**, 483-495,
740 doi:10.1111/joim.12609 (2017).
- 741 4 Evans, T., Rosenthal, E. T., Youngblom, J., Distel, D. & Hunt, T. Cyclin: a protein
742 specified by maternal mRNA in sea urchin eggs that is destroyed at each cleavage
743 division. *Cell* **33**, 389-396 (1983).
- 744 5 Nurse, P. & Thuriaux, P. Regulatory genes controlling mitosis in the fission yeast
745 *Schizosaccharomyces pombe*. *Genetics* **96**, 627-637 (1980).
- 746 6 Kittler, R. & Buchholz, F. Functional genomic analysis of cell division by
747 endoribonuclease-prepared siRNAs. *Cell Cycle* **4**, 564-567 (2005).
- 748 7 Lents, N. H. & Baldassare, J. J. RNA interference takes flight: a new RNAi screen
749 reveals cell cycle regulators in *Drosophila* cells. *Trends Endocrinol Metab* **17**, 173-174,
750 doi:10.1016/j.tem.2006.05.003 (2006).
- 751 8 Neumann, B. *et al.* Phenotypic profiling of the human genome by time-lapse
752 microscopy reveals cell division genes. *Nature* **464**, 721-727, doi:10.1038/nature08869
753 (2010).
- 754 9 McKinley, K. L. & Cheeseman, I. M. Large-Scale Analysis of CRISPR/Cas9 Cell-Cycle
755 Knockouts Reveals the Diversity of p53-Dependent Responses to Cell-Cycle Defects.
756 *Dev Cell* **40**, 405-420 e402, doi:10.1016/j.devcel.2017.01.012 (2017).
- 757 10 Pagliuca, Felicia W. *et al.* Quantitative Proteomics Reveals the Basis for the
758 Biochemical Specificity of the Cell-Cycle Machinery. *Molecular Cell* **43**, 406-417,
759 doi:10.1016/j.molcel.2011.05.031 (2011).
- 760 11 Dephoure, N. *et al.* A quantitative atlas of mitotic phosphorylation. *Proceedings of the*
761 *National Academy of Sciences of the United States of America* **105**, 10762-10767,
762 doi:10.1073/pnas.0805139105 (2008).
- 763 12 Ly, T. *et al.* A proteomic chronology of gene expression through the cell cycle in human
764 myeloid leukemia cells. *eLife* **3**, doi:10.7554/eLife.01630 (2014).
- 765 13 Bar-Joseph, Z. *et al.* Genome-wide transcriptional analysis of the human cell cycle
766 identifies genes differentially regulated in normal and cancer cells. *Proceedings of the*
767 *National Academy of Sciences* **105**, 955 (2008).
- 768 14 Dominguez, D. *et al.* A high-resolution transcriptome map of cell cycle reveals novel
769 connections between periodic genes and cancer. *Cell Res* **26**, 946-962,
770 doi:10.1038/cr.2016.84 (2016).
- 771 15 Grant, G. D. *et al.* Identification of cell cycle-regulated genes periodically expressed in
772 U2OS cells and their regulation by FOXM1 and E2F transcription factors. *Mol Biol Cell*
773 **24**, 3634-3650, doi:10.1091/mbc.E13-05-0264 (2013).
- 774 16 Pena-Diaz, J. *et al.* Transcription profiling during the cell cycle shows that a subset of
775 Polycomb-targeted genes is upregulated during DNA replication. *Nucleic Acids Res* **41**,
776 2846-2856, doi:10.1093/nar/gks1336 (2013).
- 777 17 Spellman, P. T. *et al.* Comprehensive Identification of Cell Cycle-regulated Genes of
778 the Yeast *Saccharomyces cerevisiae* by Microarray Hybridization. *Molecular Biology*
779 *of the Cell* **9**, 3273-3297 (1998).
- 780 18 Whitfield, M. L. *et al.* Identification of Genes Periodically Expressed in the Human Cell
781 Cycle and Their Expression in Tumors. *Molecular Biology of the Cell* **13**, 1977-2000,
782 doi:10.1091/mbc.02-02-0030 (2002).

- 783 19 Ishida, S. *et al.* Role for E2F in Control of Both DNA Replication and Mitotic Functions
784 as Revealed from DNA Microarray Analysis. *Molecular and Cellular Biology* **21**, 4684-
785 4699, doi:10.1128/MCB.21.14.4684-4699.2001 (2001).
- 786 20 Giotti, B., Joshi, A. & Freeman, T. C. Meta-analysis reveals conserved cell cycle
787 transcriptional network across multiple human cell types. *BMC Genomics* **18**, 30,
788 doi:10.1186/s12864-016-3435-2 (2017).
- 789 21 Balakrishnan, R., Harris, M. A., Huntley, R., Van Auken, K. & Cherry, J. M. A guide
790 to best practices for Gene Ontology (GO) manual annotation. *Database: The Journal of*
791 *Biological Databases and Curation* **2013**, doi:10.1093/database/bat054 (2013).
- 792 22 Doig, T. N. *et al.* Coexpression analysis of large cancer datasets provides insight into
793 the cellular phenotypes of the tumour microenvironment. *Bmc Genomics* **14**, doi:Artn
794 469
795 10.1186/1471-2164-14-469 (2013).
- 796 23 Theocharidis, A., van Dongen, S., Enright, A. J. & Freeman, T. C. Network
797 visualization and analysis of gene expression data using BioLayout Express3D. *Nature*
798 *Protocols* **4**, 1535-1550, doi:10.1038/nprot.2009.177 (2009).
- 799 24 Mabbott, N. A., Baillie, J. K., Hume, D. A. & Freeman, T. C. Meta-analysis of lineage-
800 specific gene expression signatures in mouse leukocyte populations. *Immunobiology*
801 **215**, 724-736, doi:10.1016/j.imbio.2010.05.012 (2010).
- 802 25 Mabbott, N. A., Baillie, J. K., Brown, H., Freeman, T. C. & Hume, D. A. An expression
803 atlas of human primary cells: inference of gene function from coexpression networks.
804 *Bmc Genomics* **14**, doi:Artn 632
805 10.1186/1471-2164-14-632 (2013).
- 806 26 Bertoli, C., Skotheim, J. M. & de Bruin, R. A. Control of cell cycle transcription during
807 G1 and S phases. *Nature reviews. Molecular cell biology* **14**, 518-528,
808 doi:10.1038/nrm3629 (2013).
- 809 27 Consortium, F. *et al.* A promoter-level mammalian expression atlas. *Nature* **507**, 462-
810 470, doi:10.1038/nature13182 (2014).
- 811 28 Brooks, R. F. Regulation of the fibroblast cell cycle by serum. *Nature* **260**, 248-250,
812 doi:10.1038/260248a0 (1976).
- 813 29 Vassilev, L. T. Cell Cycle Synchronization at the G2/M Phase Border by Reversible
814 Inhibition of CDK1. *Cell Cycle* **5**, 2555-2556, doi:10.4161/cc.5.22.3463 (2006).
- 815 30 Lizio, M. *et al.* Gateways to the FANTOM5 promoter level mammalian expression
816 atlas. *Genome biology* **16**, 22, doi:10.1186/s13059-014-0560-6 (2015).
- 817 31 Johnson, W. E., Li, C. & Rabinovic, A. Adjusting batch effects in microarray expression
818 data using empirical Bayes methods. *Biostatistics* **8**, 118-127,
819 doi:10.1093/biostatistics/kxj037 (2007).
- 820 32 Fagerberg, L. *et al.* Analysis of the human tissue-specific expression by genome-wide
821 integration of transcriptomics and antibody-based proteomics. *Mol Cell Proteomics* **13**,
822 397-406, doi:10.1074/mcp.M113.035600 (2014).
- 823 33 Enright, A. J., Van Dongen, S. & Ouzounis, C. A. An efficient algorithm for large-scale
824 detection of protein families. *Nucleic Acids Research* **30**, 1575-1584, doi:DOI
825 10.1093/nar/30.7.1575 (2002).
- 826 34 Grant, G. D. *et al.* Identification of cell cycle-regulated genes periodically expressed in
827 U2OS cells and their regulation by FOXM1 and E2F transcription factors. *Molecular*
828 *Biology of the Cell* **24**, 3634-3650, doi:10.1091/mbc.E13-05-0264 (2013).
- 829 35 Peña-Díaz, J. *et al.* Transcription profiling during the cell cycle shows that a subset of
830 Polycomb-targeted genes is upregulated during DNA replication. *Nucleic Acids*
831 *Research* **41**, 2846-2856, doi:10.1093/nar/gks1336 (2013).

- 832 36 Neumann, B. *et al.* Phenotypic profiling of the human genome by time-lapse
833 microscopy reveals cell division genes. *Nature* **464**, 721-727, doi:10.1038/nature08869
834 (2010).
- 835 37 Uhlen, M. *et al.* Towards a knowledge-based Human Protein Atlas. *Nature*
836 *Biotechnology* **28**, 1248-1250, doi:10.1038/nbt1210-1248 (2010).
- 837 38 Gene Ontology, C. Gene Ontology Consortium: going forward. *Nucleic Acids Res* **43**,
838 D1049-1056, doi:10.1093/nar/gku1179 (2015).
- 839 39 Fabregat, A. *et al.* The Reactome pathway Knowledgebase. *Nucleic Acids Research* **44**,
840 D481-D487, doi:10.1093/nar/gkv1351 (2016).
- 841 40 Blake, J. A. *et al.* Mouse Genome Database (MGD)-2017: community knowledge
842 resource for the laboratory mouse. *Nucleic acids research* **45**, D723-D729,
843 doi:10.1093/nar/gkw1040 (2017).
- 844 41 Kohler, S. *et al.* The Human Phenotype Ontology in 2017. *Nucleic acids research* **45**,
845 D865-D876, doi:10.1093/nar/gkw1039 (2017).
- 846 42 Heinz, S. *et al.* Simple combinations of lineage-determining transcription factors prime
847 cis-regulatory elements required for macrophage and B cell identities. *Molecular cell*
848 **38**, 576-589, doi:10.1016/j.molcel.2010.05.004 (2010).
- 849 43 Arenillas, D. J. *et al.* CAGED-oPOSSUM: motif enrichment analysis from CAGE-
850 derived TSSs. *Bioinformatics* **32**, 2858-2860, doi:10.1093/bioinformatics/btw337
851 (2016).
- 852 44 Zhang, J. H., Chung, T. D. Y. & Oldenburg, K. R. A simple statistical parameter for use
853 in evaluation and validation of high throughput screening assays. *Journal of*
854 *Biomolecular Screening* **4**, 67-73, doi:Doi 10.1177/108705719900400206 (1999).
- 855 45 Boutros, M., Bras, L. P. & Huber, W. Analysis of cell-based RNAi screens. *Genome*
856 *Biology* **7**, doi:ARTN R66
857 10.1186/gb-2006-7-7-r66 (2006).
- 858 46 Kittler, R., Heninger, A. K., Franke, K., Habermann, B. & Buchholz, F. Production of
859 endoribonuclease-prepared short interfering RNAs for gene silencing in mammalian
860 cells. *Nature Methods* **2**, 779-784, doi:DOI 10.1038/nmeth1005-779 (2005).
- 861 47 Kittler, R. *et al.* Genome-wide resources of endoribonuclease-prepared short interfering
862 RNAs for specific loss-of-function studies. *Nature Methods* **4**, 337-344,
863 doi:10.1038/Nmeth1025 (2007).
- 864 48 Collaboration, O. R. The ORFeome Collaboration: a genome-scale human ORF-clone
865 resource. *Nat Methods* **13**, 191-192, doi:10.1038/nmeth.3776 (2016).
- 866 49 Iyer, V. R. *et al.* The transcriptional program in the response of human fibroblasts to
867 serum. *Science* **283**, 83-87 (1999).
- 868 50 Freeman, T. C. *et al.* Construction, Visualisation, and Clustering of Transcription
869 Networks from Microarray Expression Data. *PLoS Comput Biol* **3**, e206,
870 doi:10.1371/journal.pcbi.0030206 (2007).
- 871 51 Campisi, J., Morreo, G. & Pardee, A. B. Kinetics of G1 Transit Following Brief
872 Starvation for Serum Factors. *Experimental Cell Research* **152**, 459-466, doi:Doi
873 10.1016/0014-4827(84)90647-5 (1984).
- 874 52 Chang, H. Y. *et al.* Diversity, topographic differentiation, and positional memory in
875 human fibroblasts. *Proceedings of the National Academy of Sciences of the United*
876 *States of America* **99**, 12877-12882, doi:10.1073/pnas.162488599 (2002).
- 877 53 Leone, G. *et al.* E2F3 activity is regulated during the cell cycle and is required for the
878 induction of S phase. *Genes & Development* **12**, 2120-2130, doi:DOI
879 10.1101/gad.12.14.2120 (1998).
- 880 54 Meyerson, M. & Harlow, E. Identification of G1 kinase activity for cdk6, a novel cyclin
881 D partner. *Mol Cell Biol* **14**, 2077-2086 (1994).

- 882 55 Swirski, F. K., Hilgendorf, I. & Robbins, C. S. From proliferation to proliferation:
883 monocyte lineage comes full circle. *Seminars in immunopathology* **36**, 137-148,
884 doi:10.1007/s00281-013-0409-1 (2014).
- 885 56 Fragkos, M., Ganier, O., Coulombe, P. & Mechali, M. DNA replication origin activation
886 in space and time. *Nat Rev Mol Cell Biol* **16**, 360-374, doi:10.1038/nrm4002 (2015).
- 887 57 Blomberg, I. & Hoffmann, I. Ectopic Expression of Cdc25A Accelerates the G1/S
888 Transition and Leads to Premature Activation of Cyclin E- and Cyclin A-Dependent
889 Kinases. *Molecular and Cellular Biology* **19**, 6183-6194 (1999).
- 890 58 Xu, B., Kim, S. T. & Kastan, M. B. Involvement of Brca1 in S-phase and G(2)-phase
891 checkpoints after ionizing irradiation. *Molecular and Cellular Biology* **21**, 3445-3450,
892 doi:Doi 10.1128/Mcb.21.10.3445-3450.2001 (2001).
- 893 59 Stark, G. R. & Taylor, W. R. Control of the G(2)/M transition. *Molecular Biotechnology*
894 **32**, 227-248, doi:Doi 10.1385/Mb:32:3:227 (2006).
- 895 60 Foltz, D. R. *et al.* The human CENP-A centromeric nucleosome-associated complex.
896 *Nature Cell Biology* **8**, 458-U477, doi:10.1038/ncb1397 (2006).
- 897 61 Piekorz, R. P. *et al.* The centrosomal protein TACC3 is essential for hematopoietic stem
898 cell function and genetically interfaces with p53-regulated apoptosis. *Embo Journal* **21**,
899 653-664, doi:DOI 10.1093/emboj/21.4.653 (2002).
- 900 62 Fuchs, F. *et al.* Clustering phenotype populations by genome-wide RNAi and
901 multiparametric imaging. *Molecular Systems Biology* **6**, n/a-n/a,
902 doi:10.1038/msb.2010.25 (2010).
- 903 63 Kornblum, C. *et al.* Loss-of-function mutations in MGME1 impair mtDNA replication
904 and cause multisystemic mitochondrial disease. *Nature Genetics* **45**, 214-219,
905 doi:10.1038/ng.2501 (2013).
- 906 64 Simpson, J. C., Wellenreuther, R., Poustka, A., Pepperkok, R. & Wiemann, S.
907 Systematic subcellular localization of novel proteins identified by large-scale cDNA
908 sequencing. *EMBO reports* **1**, 287-292, doi:10.1093/embo-reports/kvd058 (2000).
- 909 65 Chen, J., Bardes, E. E., Aronow, B. J. & Jegga, A. G. ToppGene Suite for gene list
910 enrichment analysis and candidate gene prioritization. *Nucleic acids research* **37**,
911 W305-311, doi:10.1093/nar/gkp427 (2009).
- 912 66 Ashburner, M. *et al.* Gene Ontology: tool for the unification of biology. *Nature Genetics*
913 **25**, 25-29 (2000).
- 914 67 Kanehisa, M. The KEGG database. *In Silico Simulation of Biological Processes* **247**,
915 91-103 (2002).
- 916 68 Iyer, V. R. *et al.* The transcriptional program in the response of human fibroblasts to
917 serum. *Science* **283**, 83-87 (1999).
- 918 69 Zhang, C. *et al.* PRR11 regulates late-S to G2/M phase progression and induces
919 premature chromatin condensation (PCC). *Biochemical and biophysical research*
920 *communications* **458**, 501-508, doi:10.1016/j.bbrc.2015.01.139 (2015).
- 921 70 Morenos, L. *et al.* Hypermethylation and down-regulation of DLEU2 in paediatric acute
922 myeloid leukaemia independent of embedded tumour suppressor miR-15a/16-1. *Mol*
923 *Cancer* **13**, 123, doi:10.1186/1476-4598-13-123 (2014).
- 924 71 Wang, L. L. *et al.* DLEU1 contributes to ovarian carcinoma tumourigenesis and
925 development by interacting with miR-490-3p and altering CDK1 expression. *J Cell Mol*
926 *Med*, doi:10.1111/jcmm.13217 (2017).
- 927 72 Forsberg, J., Zhivotovsky, B. & Olsson, M. Caspase-2: an orphan enzyme out of the
928 shadows. *Oncogene*, doi:10.1038/onc.2017.169 (2017).
- 929 73 Dawar, S. *et al.* Caspase-2-mediated cell death is required for deleting aneuploid cells.
930 *Oncogene* **36**, 2704-2714, doi:10.1038/onc.2016.423 (2017).

- 931 74 Vitale, I., Manic, G., Castedo, M. & Kroemer, G. Caspase 2 in mitotic catastrophe: The
932 terminator of aneuploid and tetraploid cells. *Mol Cell Oncol* **4**, e1299274,
933 doi:10.1080/23723556.2017.1299274 (2017).
- 934 75 Doxsey, S., Zimmerman, W. & Mikule, K. Centrosome control of the cell cycle. *Trends*
935 *in Cell Biology* **15**, 303-311, doi:10.1016/j.tcb.2005.04.008 (2005).
- 936 76 Gupta, G. D. *et al.* A Dynamic Protein Interaction Landscape of the Human
937 Centrosome-Cilium Interface. *Cell* **163**, 1484-1499, doi:10.1016/j.cell.2015.10.065
938 (2015).
- 939 77 Snyder, M., He, W. & Zhang, J. J. The DNA replication factor MCM5 is essential for
940 Stat1-mediated transcriptional activation. *Proceedings of the National Academy of*
941 *Sciences of the United States of America* **102**, 14539-14544,
942 doi:10.1073/pnas.0507479102 (2005).
- 943 78 DaFonseca, C. J., Shu, F. & Zhang, J. J. Identification of two residues in MCM5 critical
944 for the assembly of MCM complexes and Stat1-mediated transcription activation in
945 response to IFN-gamma. *Proc Natl Acad Sci U S A* **98**, 3034-3039,
946 doi:10.1073/pnas.061487598 (2001).
947
948